Decadal-Scale Temperature Trends in the Southern Hemisphere Ocean

SARAH T. GILLE

Scripps Institution of Oceanography, and Department of Mechanical and Aerospace Engineering, University of California, San Diego, La Jolla, California

(Manuscript received 2 July 2007, in final form 13 February 2008)

ABSTRACT

Long-term trends in the heat content of the Southern Hemisphere ocean are evaluated by comparing temperature profiles collected during the 1990s with profiles collected starting in the 1930s. Data are drawn both from ship-based hydrographic surveys and from autonomous floats. Results show that the upper 1000 m of the Southern Hemisphere ocean has warmed substantially during this time period at all depths. Warming is concentrated within the Antarctic Circumpolar Current (ACC). On a global scale, this warming trend implies that the ocean has gained heat from the atmosphere over the last 50 to 70 years. Although the data do not preclude the possibility that the Southern Ocean has warmed as a result of increased heat fluxes, either into the ocean or within the ocean, in general the strong trend in the Southern Ocean appears regionally consistent with a poleward migration of the ACC, possibly driven by long-term poleward shifts in the winds of the region, as represented by the southern annular mode.

1. Introduction

The Southern Ocean is a sparsely sampled section of the global oceans. Not only is it large and accessible from only a few ports, but it is also an inhospitable environment, with high sea states forced by the strongest winds in the world. As a result, temperature data collected by research vessels over the past few decades contain numerous gaps, which impede assessment of Southern Ocean and overall Southern Hemisphere temperature change. Southern Hemisphere uncertainties are nearly twice as large as Northern Hemisphere uncertainties for estimates of increase in global ocean heat content since the 1950s (e.g., Levitus et al. 2000, 2005a; Harrison and Carson 2007).

The Southern Ocean plays an important role in the climate system for a number of reasons. First, it is a region of strongly tilted isopycnals. Isopycnal surfaces that outcrop to the surface at 60°S can descend to depths greater than 1500 m at 40°S (see, e.g., Gouretski and Jancke 1998), providing a ready conduit to carry heat and other tracers from the surface into the mid-depth ocean. Because of this rapid exchange with the deep ocean, coupled with cold surface waters and strong winds, the Southern Ocean is expected to be a prime region for CO_2 uptake, although not necessarily for CO_2 storage (Caldeira and Duffy 2000; Sabine et al. 2004). The heat content of the upper Southern Ocean, as well as meridional heat transport through the Southern Ocean and regional air–sea heat fluxes, may influence (and respond to) atmospheric temperatures. Temperature records of 30- to 50-yr duration from the Antarctic Peninsula indicate surface air temperature trends of 3.3° to 5.6°C per century (see supplementary material of Vaughan et al. 2001), though temperatures in the interior of the Antarctic continent appear not to show a statistically significant warming trend during the same time period (e.g., Doran et al. 2002; Chapman and Walsh 2007). This temperature rise is associated both with increased upper ocean temperatures (Meredith and King 2005) and with the retreat of ice shelves on the Antarctic Peninsula (Vaughan and Doake 1996; Pritchard and Vaughan 2007), and some studies have speculated that anomalously warm subsurface ocean temperatures near the ice shelves are also a factor in ice shelf bottom melt rates (e.g., Rignot and Jacobs 2002; Jacobs 2006). To the extent that retreating ice shelves are linked to continental ice storage, they also imply an increase in global sea level (Munk 2003), with far-reaching consequences in coastal areas.

Modeling studies have suggested that the Southern

Corresponding author address: Sarah T. Gille, Scripps Institution of Oceanography, University of California, San Diego, La Jolla, CA 92093-0230.
E-mail: sgille@ucsd.edu

DOI: 10.1175/2008JCLI2131.1

Ocean should respond rapidly to climate change. Using the Hadley Centre climate model, Banks and Wood (2002) predicted that after 30 years of anthropogenic greenhouse gas forcing, warming should be detectable in the upper 1500 m of the Southern Ocean. Similarly, on the basis of South Atlantic results from the National Center for Atmospheric Research Community Climate System Model, Wainer et al. (2004) suggested that a global warming scenario would yield rapid changes in SST and barotropic transport within the Antarctic Circumpolar Current (ACC) compared with the subtropical gyres to the north. The ensemble of coupled climate simulations run as part of the Intergovernmental Panel on Climate Change Fourth Assessment Report generally shows significant warming within the Southern Ocean (e.g., Fyfe and Saenko 2005, 2006). These model predictions appear to be supported by a number of limited observational studies. Regional studies (e.g., Aoki et al. 2003; Sprintall 2008) and data collected north of the Southern Ocean also support the idea that the Southern Ocean may be undergoing rapid climate change. In analyses of midlatitude hydrographic sections, Wong et al. (2001) and Arbic and Owens (2001) found that waters ventilated in the Southern Ocean appeared to have changed significantly during recent decades. Gille (2002) expanded on the work of Levitus et al. (2000) by comparing hydrographic temperature data with temperature data collected during the 1990s by Autonomous Lagrangian Circulation Explorer (ALACE) floats at depths between 700 and 1100 m, the "parking depths" of the floats. That analysis implied that middepth Southern Ocean temperatures rose by nearly 0.2°C between the 1950s and the 1990s, a rate that was double the global prediction obtained by Levitus et al. (2000) for the upper 1000 m and comparable to atmospheric warming in the same latitude band.

This study extends the work of Gille (2002) by examining long-term temperature change throughout the upper 1000 m. Like the previous work, this analysis compares 1990s observations with historic hydrographic observations collected in the same geographic area to obtain estimates of decadal-scale temperature changes within the Southern Ocean and throughout the Southern Hemisphere. Hydrographic observations made from ships are used as well as measurements from autonomous Argo and Profiling ALACE (PALACE) floats. Section 2 discusses the observations used in this analysis. Temperature changes are presented in section 3, their geographic patterns in section 4, and their implications in section 5. Section 6 explores mechanisms that may be responsible for these changes. Finally, results are summarized in section 7.

2. Southern Hemisphere observations

a. Data

The float and hydrographic datasets used for this study are publicly available. All provide temperature profiles within the top kilometer of the water column.

The hydrographic data come from the *World Ocean Database 2005* (*WOD05*) (Boyer et al. 2006). *WOD05* was selected because it represents a fairly complete, quality-controlled compilation of all available observations including numerous records that were not in earlier versions of the *World Ocean Database*. The earliest observations in *WOD05* date from the late nineteenth century, but this analysis is confined to data collected starting in the 1930s. Temperature observations include measurements from expendable bathythermographs (XBT), bottle data (OSD), and conductivity–temperature–depth probes (CTD). Data collection technology has evolved over time; everything collected prior to 1970 came from OSD, while more recent observations are primarily from XBTs and CTDs. Recent field programs have often collected CTD and OSD data at the same locations using a standard CTD with rosette. To avoid duplications, here OSD data are eliminated if they were collected within 0.9 km and within 3 h of a CTD station. *WOD05* also includes mechanical bathythermograph data (MBT), but these have been omitted from this analysis for reasons discussed in the appendix. This analysis made use of temperature data from standard depths of 10, 20, 30, 50, 75, 100, 125, 150, 200, 250, 300, 400, 500, 600, 700, 800, 900, 1000, and 1100 m. To ensure consistency in this analysis, temperatures are converted to potential temperature.

Quality flags identify observations that differ by more than three standard deviations (in the open ocean) from annual, seasonal, or monthly regional averages. For this analysis, data were discarded if they failed two or more of these standard deviation tests (corresponding to a quality flag of six or more in *WOD05*) (Johnson et al. 2006). The database has undergone several minor revisions since its initial release; data used in this analysis were downloaded in September 2006.

PALACE floats began collecting upper-ocean temperature profiles during the 1990s as part of the World Ocean Circulation Experiment (WOCE) (Davis et al. 1992, 2001), and their successors, Argo floats, formally began operation in 1997 (Roemmich et al. 2001). PALACE and Argo data are included in *WOD05* but here have been drawn from separate sources so as to include up-to-date files. R. Davis (Scripps Institution of Oceanography) provided the PALACE data, and Argo

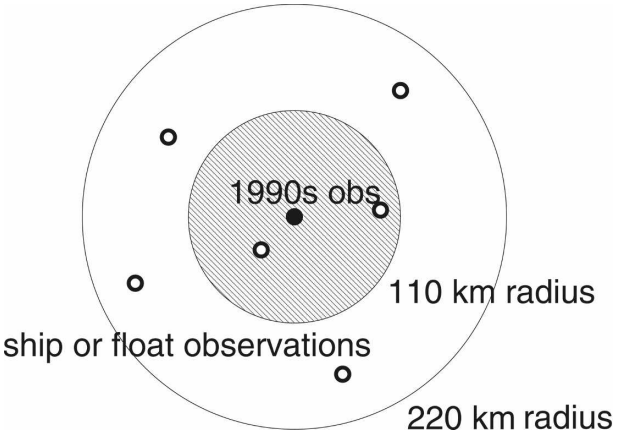

FIG. 1. Schematic illustrating strategy for identifying nearest neighbor data pairs. For each float, CTD, XBT, or bottle profile position collected during the 1990s (represented by the solid black dot), all observations within a 220-km radius (open circles) are identified. For reference, the cross-hatched region defines distances less than 110 km (or 1° latitude).

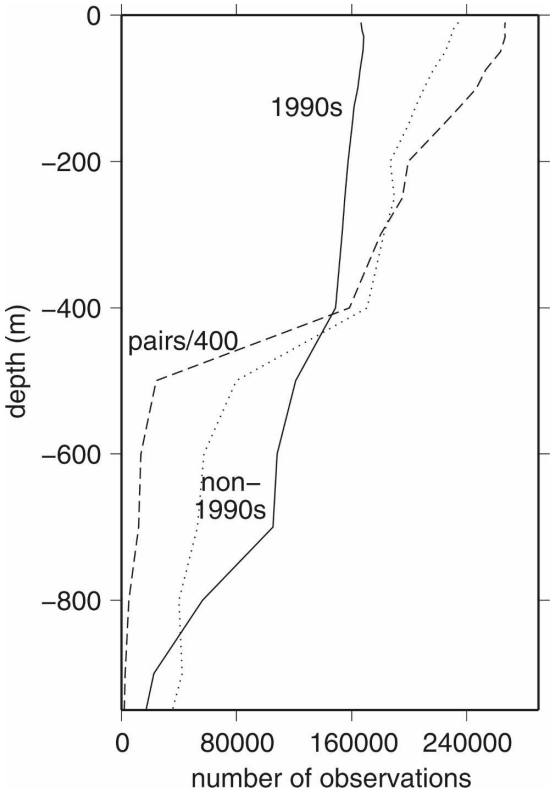

FIG. 2. Number of 1990s observations (solid line), comparison observations from before or after the 1990s (dotted line), and data pairs divided by 400 (dashed line) as a function of depth. Pairs of profiles are only selected for this analysis if they are within 220 km of each other, and in this plot all pairs are separated in time by at least 10 yr.

data were drawn directly from the Argo Global Data Assembly Center. PALACE and Argo data have been used for a variety of different types of studies of ocean circulation and climatology (e.g., Davis et al. 1996; Davis 1998; Lavender et al. 2000; Gille 2003; Davis 2005). The floats follow ocean currents at depths typically between about 700 and 1100 m for 9 to 25 days, then rise to the ocean surface to transmit their data to satellite. As they rise to the ocean surface, they record a temperature profile. PALACE profiles are transmitted with 5–8 dbar vertical resolution in the upper ocean, 8–10-dbar vertical resolution between 300 and 800 dbar, and 16–20-dbar vertical resolution between 800 m and the bottom of the profiles. Argo profiles use a similar standard. Pressures are accurate to approximately ±5 dbars. The floats were equipped with calibrated temperature sensors like those used on modern CTDs. Unlike CTDs, floats cannot be recovered and recalibrated, but they are expected to provide temperatures with roughly 0.01°C accuracy.

Float data were checked for obvious errors, and data on the Argo gray list and flagged data are not included in this analysis. For this study, PALACE and Argo measured pressures were converted to depths (Saunders and Fofonoff 1976), temperatures were converted to potential temperature, and observations were linearly interpolated to provide temperature estimates at each of the *WOD05* standard depths.

Data were selected for this analysis if they were collected within 220 km (a distance equivalent to 2° latitude) of any profile collected during the 1990s. Figure 1 illustrates the strategy used to identify nearest neighbor pairs. The resulting database includes as many as 150 000 observations from the 1990s paired with more than 202 000 earlier and later observations to produce a maximum of 143×10^6 pairs. Figure 2 depicts the number of observations as a function of depth. Many of the XBT observations extend only to 400-m depth, which accounts for the sharp drop in available data below 400 m. Figure 3 shows the geographic distribution of the observations at 500-m depth available for this study. The upper panel indicates positions of 1990s data, color coded by instrument type. The lower panel shows how the spatial coverage has changed over time with recent data (red) coming largely from floats that sample somewhat randomly in space and older data more often concentrated in coastal regions or on long sections. Although the number of observations varies with depth, the geographic distribution is similar at all depths. In the Southern Ocean hydrographic observations are densest near Drake Passage, while float observations are distributed circumpolarly.

Seasonal variability is expected to the depth of the

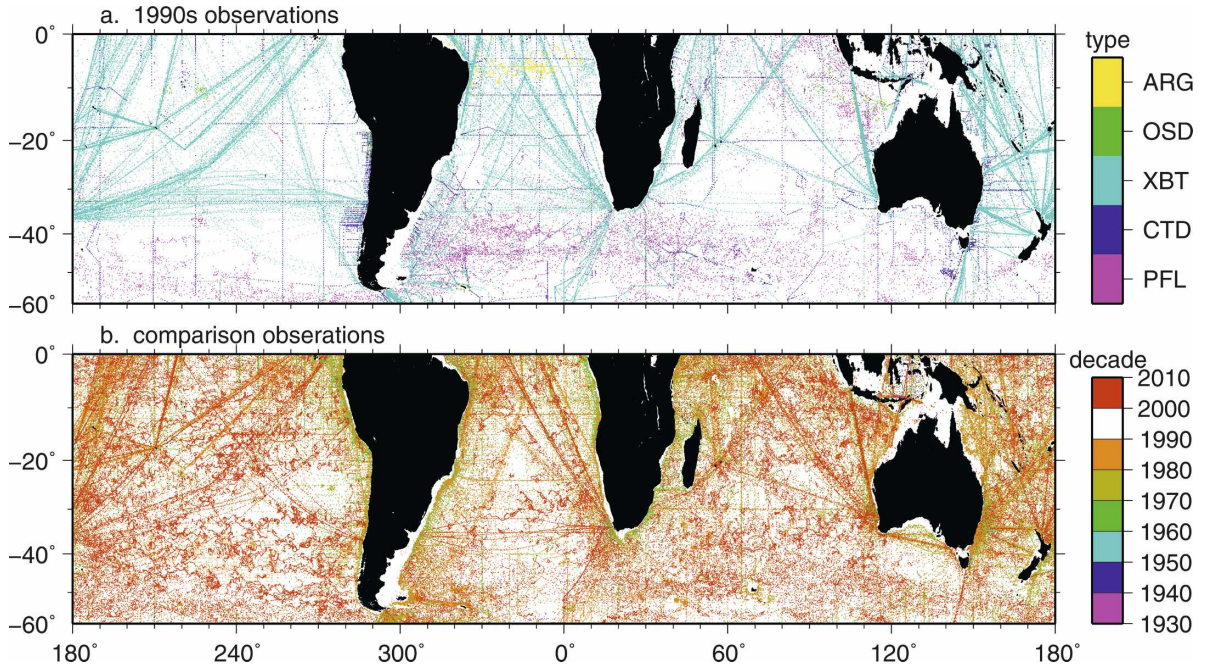

FIG. 3. Geographic distribution of observations at 500-m depth available for this study. (top) Observations collected during the 1990s, color-coded by data type; (bottom) non-1990s observations, color-coded by decade. Float and hydrographic observations are used only if they can be paired with each other using a 220-km search radius, so not all plotted data points can be paired with another observation to be incorporated into the temperature trend analysis.

seasonal thermocline, often estimated to be 100 to 200 m deep at midlatitudes (e.g., Pickard and Emery 1990; Capotondi et al. 2005) though deeper influences might be expected in the mode-water formation regions of the Southern Ocean. Since most Southern Ocean shipboard observations are carried out only during summer months, while float and Drake Passage XBTs operate steadily throughout the year, there are clear seasonal biases in the data that could lead to systematic temperature differences, at least within the upper part of the water column. In principle, the seasonal bias could be removed by correcting for a seasonal cycle only in the upper ocean (e.g., Gouretski and Koltermann 2007) but, because of the paucity of winter observations in the Southern Ocean, here the seasonal effect is minimized by confining the analysis to data collected between November and March, nominally during the Southern Hemisphere summer. (Historically, Southern Ocean observations were collected unevenly during summer months, with more observations concentrated between January and March. The use of the 5-month time window allows more data to be used in this analysis than would be available if a 3-month window were used, but it cannot entirely remove seasonal effects.) No systematic biases between different instrument types are apparent in this analysis, although there are detectable differences, as discussed in the appendix.

b. Minimizing impact of spatial sampling

Geographic differences between measurement sites can also lead to temperature differences, particularly near large temperature fronts such as western boundary currents or the ACC. However, random geographic differences do not necessarily imply systematic temperature biases, and in this analysis geographic effects are assumed to be a source of noise rather than bias.

Systematic biases in data sampling are a more serious concern for this analysis. Temperature trend results can be extremely sensitive to the methods used to "infill" regions with no observations (e.g., AchutaRao et al. 2006; Gregory et al. 2004; Gouretski and Koltermann 2007). The data distributions in Fig. 3 suggest that historical data coverage is not particularly uniform in time or space. Observational programs have carried out repeated observations in the tropics and along primary shipping routes, but regions such as the southeastern Pacific, the southern Indian Ocean, and the Southern Ocean have been sampled less frequently in the historical database. A simple nearest neighbor comparison that gives equal weight to each individual observation would therefore be a measure primarily of temperature changes in well-sampled parts of the ocean. To avoid weighting the analysis strictly by the number of available observations, this analysis sorts data pairs into geo-

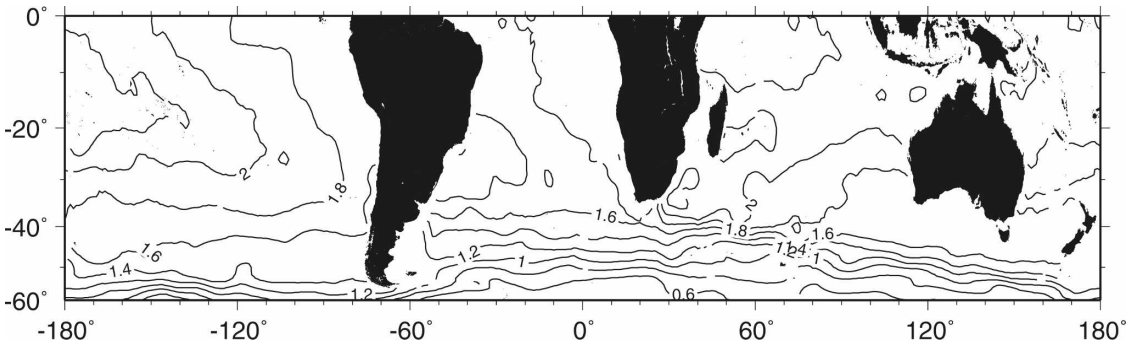

FIG. 4. Dynamic height at the surface relative to 1500 m computed from the Gouretski and Jancke (1998) atlas.

graphic bins before computing average temperature changes. Three different types of geographic bins are used: 1) Latitudinal bins are defined in 10° latitudinal segments between 60°S and the equator. These have the merit of being easy to define but the disadvantage that they combine disparate oceanographic regions that may experience different long-term trends, such as western boundary currents and ocean interior areas. 2) As an alternative, smaller 5° latitude by 5° longitude bins are also used. These resolve substantial spatial variability but include many geographic bins containing no observations, particularly deep in the water column. In this analysis 5° by 5° bins that contain no data at a given depth are assumed either to have experienced no change at that depth or to have experienced a change equivalent to the mean change of bins at that depth that do contain data. 3) To account for different dynamical regions, while also ensuring the availability of multiple observations in each bin, bins are also defined in 0.2 dynamic meter increments from dynamic topography at the surface relative to 1500 m (see Fig. 4), computed from the Gouretski and Jancke (1998) atlas. These bins have the disadvantage of being highly variable in size, and during some decades no observations were collected in some of the nominal bins. In addition to these three weighting strategies, a "no-averaging" option is also considered in which each observational pair is given equal weight.

Each data pair consists of a 1990s reference observation and a nonreference historic observation collected any time between 1930 and 2006. In addition to sorting pairs by geographic bin, they are also sorted by decade of observation of the historic observation. In each geographic and decadal bin, mean temperature differences and statistical uncertainties are computed. These are then weighted by the geographic area occupied by each dynamic height region to obtain mean temperature and heat content trends for the entire Southern Hemisphere.

3. Temperature and heat content changes

Figure 5 indicates mean differences between reference temperature profiles from the 1990s and profiles collected throughout the historic record. Few data are available from the 1940s, which accounts for the large error bars associated with 1990s minus 1940s profiles. The profiles suggest that the Southern Hemisphere ocean has warmed progressively during the time period between the 1930s and the 1990s. Warming appears intensified near the surface but is statistically significant at all depths where the comparisons can be made.

The temperature profiles in Fig. 5 imply a net in-

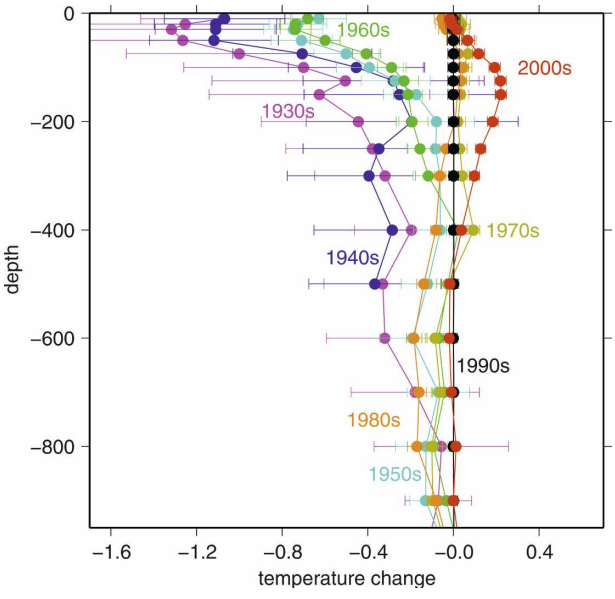

FIG. 5. Profiles of temperature difference between 1990s temperature profiles and hydrographic data sorted by decade. Differences are computed as 1990s reference temperatures minus historic temperature profiles sorted by decade, using the nearest neighbor method discussed in the text. Here results are presented for summer data (November through March), averaged first by latitude band.

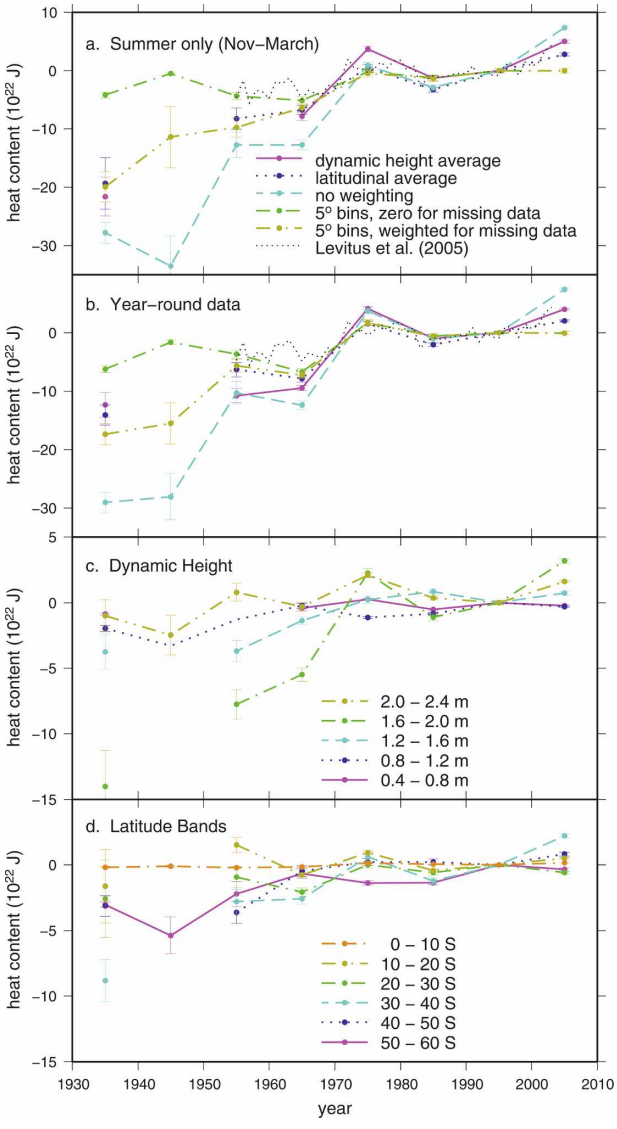

FIG. 6. (a) Changes in upper ocean heat content for top 700 m determined from differences between 1990s and historic temperature profiles using summertime only data, averaged by dynamic height contour (solid magenta line), by latitude band (dotted blue line), with no geographic weighting (dashed cyan line), by 5° by 5° bins with zero trend assumed for bins with no data (dashed–dotted green line), or in 5° by 5° bins with bins without data assumed to have the average trend (dashed–double-dotted gold line). (b) As in (a) but using data collected throughout the year. In both cases, error bars represent two standard deviation statistical standard errors. (c) Changes in summertime upper-ocean heat content, subdivided regionally based on dynamic height contour (as shown in Fig. 4). (d) As in (c) but subdivided regionally based on latitude.

crease in upper ocean heat since the 1930s. Figures 6a and 6b show time series of the vertical integral of the temperature profiles over the top 700 m of the ocean, represented as a change in Southern Hemisphere heat content. [The 700-m depth range is selected to facilitate comparison with the Levitus et al. (2005a) findings.] Here results determined using each of the averaging methods described in section 2 are plotted, as described in the caption and legend to Fig. 6a. In addition, Table 1 summarizes the net changes between the 1930s and the present and between the 1950s and the present for each of these scenarios.

The analysis indicates substantial increases in Southern Ocean heat content over the last 50 to 70 yr exceeding the formal measurement uncertainties, although the results are sensitive to the choice of binning method. For summer and year-round data, trends are largest in the no-averaging scenario (dashed cyan lines in Figs. 6a,b), presumably because regions that can undergo rapid and significant change, such as frontal regions, also tend to be well sampled. This trend is strongly influenced by temperature differences in the upper 200 m of the ocean. Trends are smallest when data are averaged in 5° by 5° bins assuming zero trend in bins with missing data (dashed–dotted green lines in Figs. 6a,b). Comparable trends of intermediate magnitude are found for the three other averaging methods, based on bins defined by dynamic height range (magenta solid lines), 10° latitudinal bins (blue dotted lines), or 5° by 5° bins with empty bins assumed to have average trends (dashed–double-dotted gold lines).

Summer-only results (Fig. 6a) systematically show a larger trend than year-round results (Fig. 6b, see also Table 1). This is not surprising since, as noted above, the 1990s reference observations include large numbers of year-round observations from the float and XBT programs, while historic observations are biased to summer months. The year-round analysis is typically able to make use of twice as many observations and five times more data pairs than the summer-only analysis. (Even though historically fewer observations have been collected in winter months, the large increase in data comes because more nearest neighbor matches are found for each individual observation.) However, because of the potential biases associated with a year-round analysis, particularly in the upper ocean, the summertime results have been assumed to be more representative of net long-term changes in the ocean.

The trends found here using summer data in latitudinal bins, dynamic height bins, or 5° by 5° bins (with missing data assumed to have a mean trend) suggest a 10 to 11 $\pm$ 2 ($\times 10^{22}$ J) heat content rise from the 1950s to the present (see Table 1). This is roughly double the net heat content increase of 5.4×10^{22} J reported by Levitus et al. (2005a). In this analysis, the Levitus et al. increase can be duplicated only if year-round data are used (Fig. 6b), or if summer data are used but zero

TABLE 1. Mean heat content rise (10^{22} J) between the 1930s and the present in upper 700 m of the ocean (following Levitus et al. 2005a). Error bars nominally represent two standard deviation errors.

Method	1930s to present		1950s to present	
	Summer	Year-round	Summer	Year-round
No averaging	35 ± 2	37 ± 2	20 ± 2	18 ± 2
Dynamic height bins	27 ± 3	16 ± 2	—	15 ± 1
10° latitude bins	22 ± 4	16 ± 2	11 ± 2	8 ± 1
5° × 5° bins (no data = mean trend)	20 ± 3	17 ± 2	10 ± 2	6 ± 1
5° × 5° bins (no data = zero trend)	4.2 ± 0.7	6.2 ± 0.7	4.3 ± 0.8	3.6 ± 0.8
Levitus et al. (2005a)				5.4

trend is assumed in 5° × 5° bins with no data (dashed–dotted green line in Fig. 6a). The methodology of Levitus et al. (2001, 2005a) essentially makes both these assumptions: they combined year-round data and they mapped temperature anomalies by assuming no net change in heat content in regions for which no observations are available (Conkright et al. 2002; Locarnini et al. 2006). This strategy is likely to underrepresent heat content changes in the high-latitude Southern Ocean, where observations are particularly sparse. As statistical studies have often pointed out, mapped data fields can be very sensitive to a priori guesses about the structure of the data (e.g., Bretherton et al. 1976); in this case, as also noted by Gouretski and Koltermann (2007), there is a clear distinction between assuming that poorly sampled parts of the ocean have experienced zero trend and assuming a priori that poorly sampled parts of the ocean have experienced a trend typical of better sampled regions.

Although the observed heat content increase appears to have been concentrated in the upper ocean, it extends below the 700-m range considered here. In this analysis, total heat content rise for the top 1050 m of the ocean averages 19%–25% higher in the time ranges considered here. From 1955 through 2003, Levitus et al. (2005a) showed a net increase in Southern Hemisphere ocean heat content of 7.2×10^{22} J for the upper 3000 m of the ocean, implying a 1.8×10^{22} J increase between 3000 and 700 m. Within the upper 3000 m, Gouretski and Koltermann (2007) found a larger increase of $12.8 \pm 8.0 \times 10^{22}$ J for the time period between 1957–66 and 1987–96. This dropped to $4.3 \pm 8.0 \times 10^{22}$ J if only CTD and bottle data were used. They did not report trends for the upper 700 m alone.

Results reported here use all 1990s observations as reference values. Since XBT data dominate the recent records and are collected primarily along specific shipping routes, they could potentially bias the results. Therefore, trends were also computed using only float or XBT observations as 1990s reference values. While the quantitative estimates of heat content change are sensitive to the choice of reference data, the overall trend patterns between the 1950s and the present are consistent, regardless of reference data. In particular, despite the reported warm bias in XBT data (Gouretski and Koltermann 2007), excluding XBT data from this analysis did not systematically increase or decrease the heat content trend.

4. Geographic patterns in heat content change

The long-term temperature rise documented in Figs. 5 and 6a,b has not occurred uniformly throughout the Southern Hemisphere. The lower panels of Fig. 6 show heat content rise since the 1930s, plotted separately for different dynamic height ranges (Fig. 6c) and for different latitude bands (Fig. 6d). Regions defined on the basis of dynamic height contours vary enormously in size, as Fig. 4 indicates, and not surprisingly, in Fig. 6c, the largest heat content increase is associated with the dynamic height range from 1.6 to 2.0 dynamic meters, which also occupies the largest surface area. Latitudinal bands are more nearly equal in size, and Fig. 6c shows that between 20°S and the equator, there has been little net change in ocean heat content since the start of this analysis. From the 1930s to the present, 80% of the net increase in Southern Hemisphere ocean heat content occurred south of 30°S. From 1955 through 2005, essentially all of the increase appears to be south of 30°S, with 83% between 30° and 50°S and 17% between 50° and 60°S.

Overall, depths below 175 m account for only 43% of the heat content change between the mid-1950s and the present (not shown). However, these depths play a larger role in heat content trends at high latitudes, accounting for 75% of the change between 50° and 60°S and for 69% of the change between 40° and 50°S. One possible explanation for the significant warming in the deep high-latitude ocean is that the regional combination of deep seasonal mixed layers, low stratification, and advection along steeply tilted isopycnals together

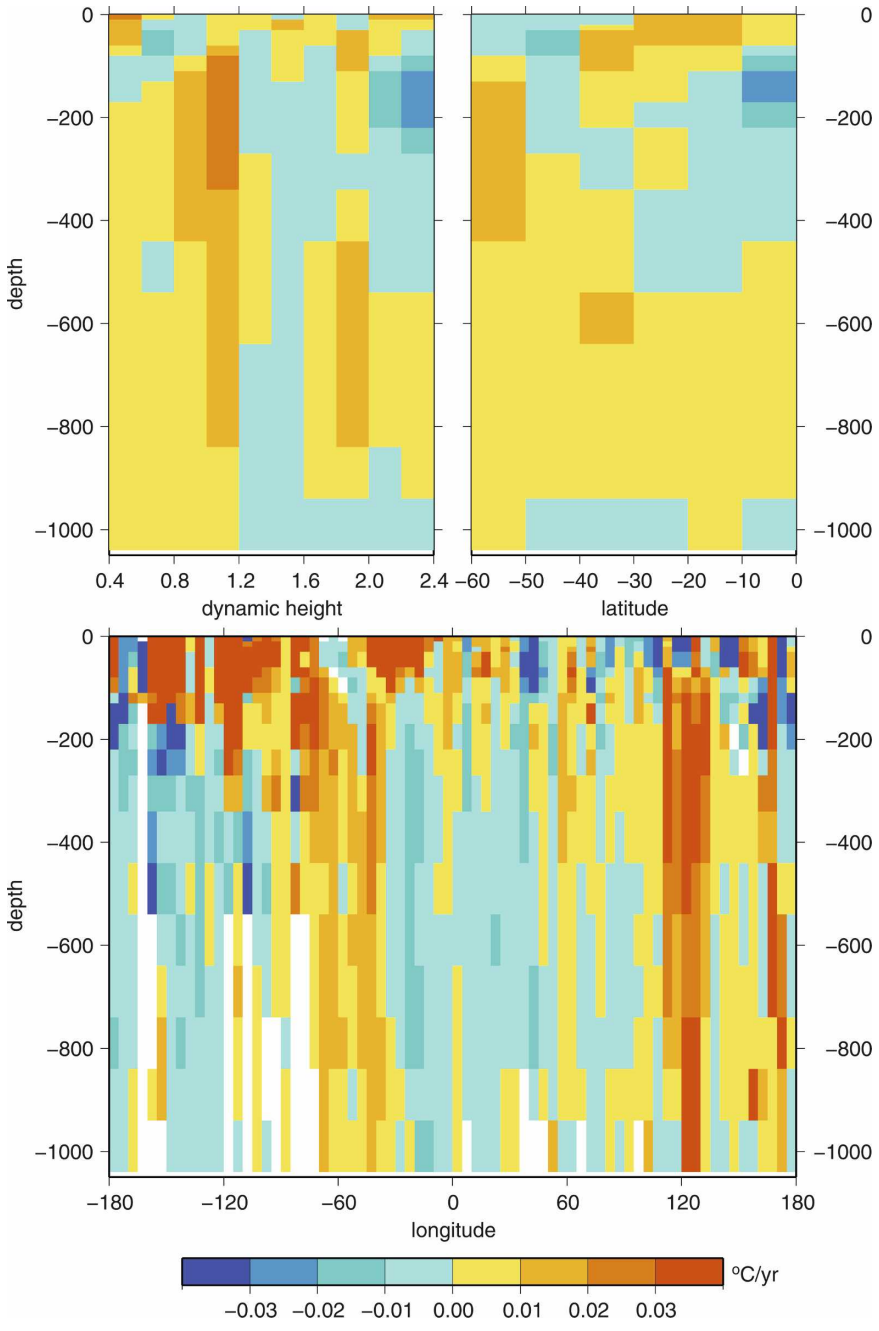

FIG. 7. (top left) Rate of change of temperature averaged as a function of dynamic height for summer months only. Summer month rate of temperature change (top right) as a function of latitude and (bottom) between 55° and 60°S as a function of longitude. White areas indicate regions where the average trends are not statistically different from zero.

allow temperature changes to penetrate rapidly below the surface layer of the ocean.

Figure 7 shows the rate of change of summertime temperatures within regions defined by dynamic height contour (top left panel), by latitude (top right panel), and by longitude (bottom panel). Here, to avoid biasing the results with short-term processes, rates of change are computed using only data pairs that are separated in time by at least 10 yr. These rates are then averaged within bins defined either by surface dynamic topography or latitude. Since mean rates of change are not computed in the same way as the heat content values in

Fig. 6, they will not necessarily show warming occurring in precisely identical regions.

The top left panel of Fig. 7 indicates rapid temperature trends at nearly all depths for dynamic contours lower than 1.2 dynamic meters, corresponding roughly to the region that makes up the ACC. The apparent cooling in the upper 100 to 200 m of the ACC is not apparent in long-term reconstructions of sea surface temperature (Smith and Reynolds 2004) and may be an artifact of the improved 1990s sampling, which includes more observations in early and late summer. This cooling becomes more pronounced if year-round data are considered (not shown). The annual cycle of SST in this region has an amplitude of 1° to 2°C (Reynolds and Smith 1994) and the apparent cooling trend is roughly consistent with the trend that would be expected as a result of changes in seasonal sampling. North of the ACC, large rates of temperature change are confined largely to the upper 100 m of the ocean, and this analysis suggests slight cooling between 100- and 500-m depth for most dynamic height values.

The top right panel of Fig. 7 shows warming trends as a function of latitude. In this coordinate system, rapid subsurface warming appears to have occurred below 100-m depth south of 50°S, and between 500 and 900 m at latitudes from 20° to 40°S. Upper-ocean warming rates are largest between 10° and 40°S.

Temperature trends are noisier and more difficult to interpret when they are computed in 5° by 5° bins. The bottom panel of Fig. 7 shows warming trends, as a function of longitude, within the latitude band between 55° and 60°S. Subsurface warming is evident over a broad range of longitudes, but near-surface warming is more clearly evident between about 160°W and 30°E, corresponding to the Pacific and Atlantic sectors. Within many of the other latitude bands (not shown), near-surface cooling occurs in the Indian Ocean and may reflect any of several factors: differences in the historical sampling of the Indian Ocean compared with other basins, differences in the observing systems, or genuine climatic differences.

Taken together, these results suggest that in the latitude band containing the ACC, the top 1000 m of the ocean have undergone substantial warming since the 1950s, that most of the heat content change in the Southern Hemisphere since the 1950s has occurred poleward of 30°S, and that any changes that have occurred in the tropics are largely confined to the surface mixed layer and have had comparatively less impact on global ocean heat content. The next sections will explore the implications of these results and the possible mechanisms that may govern these temperature changes.

5. Implications

a. Sea level change

Since the density of seawater decreases when the water warms, increases in ocean heat content translate into increases in global sea level due to steric expansion (e.g., Cazenave and Nerem 2004; Levitus et al. 2005b; Bindoff et al. 2007). Previous analyses of World Ocean Atlas data indicate a thermosteric sea level increase of 0.31 ± 0.07 mm yr^{-1} (Ishii et al. 2006) to 0.33 ± 0.04 mm yr^{-1} (Antonov et al. 2002, 2005) for the upper 700 m of the ocean between 1955 and 2003, with a slightly larger increase of 0.40 ± 0.05 mm yr^{-1} when the top 3000 m of the ocean are considered (Antonov et al. 2005; Bindoff et al. 2007). Ocean general circulation models imply a total steric expansion of 0.3 to 0.7 mm yr^{-1} (Church et al. 2001). Sea level rise appears to have accelerated in the latter part of the twentieth century (Church and White 2006), but that will not be considered here because of the coarse temporal sampling used in this analysis. Long-term changes in ocean salinity can also contribute to steric sea level change (Ishii et al. 2006), and these effects, while expected to be small, are also not considered here because of the limited availability of historic salinity data. Observed twentieth-century sea level rise appears to have exceeded the estimates obtained by summing individual contributions due to steric expansion of the ocean, continental ice melt, terrestrial water storage, and postglacial rebound (Munk 2002; Nerem et al. 2006), with the total imbalance estimated at about 0.7 ± 0.7 mm yr^{-1} (Bindoff et al. 2007), and one open question is whether hydrographic sampling issues may have contributed to this apparent imbalance.

In this analysis, trends in thermosteric sea level are computed using a method similar to that described by Antonov et al. (2002). Thermal expansion coefficients were determined from the World Ocean Atlas climatology (Locarnini et al. 2006) as a function of latitude, longitude, and depth. These were applied to each data pair before averaging to obtain a mean change in dynamic height, sorted by bins as before. The results are summarized in Table 2, with trends computed two different ways. Following Levitus et al. (2005b), trends in the right column were computed from a weighted least squares fit for the interval from the 1930s to the 1990s. Here the present decade is omitted, because data are by necessity all concentrated in the first half of the decade. Because error bars are large in the first

TABLE 2. Mean rate of thermosteric sea level rise (mm yr^{-1}) from the 1930s to the present in upper 700 m of the ocean, using summer data only (following Antonov et al. 2005; Levitus et al. 2005b). Error bars nominally represent two standard deviation errors.

Method	1930s to present	
	Least squares fit	Total trend
No averaging	1.23 ± 0.05	1.44 ± 0.07
Dynamic height bins	0.40 ± 0.05	1.18 ± 0.14
10° latitude bins	0.59 ± 0.05	1.24 ± 0.22
5° × 5° bins (no data = mean trend)	0.48 ± 0.06	0.57 ± 0.09
5° × 5° bins (no data = zero trend)	0.07 ± 0.02	0.13 ± 0.02
Antonov et al. (2005)		0.33 ± 0.04

part of the record, the weighted fit is based largely on post-1950s observations. In the right column, the trend has been determined using the simple difference between present decade and 1930s dynamic height anomalies. Sea surface rise estimates are sensitive to the analysis approach. For example, a least squares fit for the case using 10° latitudinal averages suggests a trend of 0.59 ± 0.05 mm yr^{-1}, while dynamic height bins imply a trend of 0.40 ± 0.05 mm yr^{-1}, both significantly larger than the 0.33 ± 0.04 mm yr^{-1} trend inferred by Antonov et al. (2005) for the top 700 m. As the heat content changes summarized in Table 1 suggest, the increase in thermal expansion relative to previous studies can be attributed in part to the focus on summer-only data and in part to the statistical assumptions made about times and places with no observations.

If we assume that the Antonov et al. (2005) results are consistent for depths from 3000 to 700 m but substitute these results in for the top 700 m, this implies a total rate of thermosteric sea level rise of at least 0.47 to 0.66 (±0.06) mm yr^{-1} during the second half of the twentieth century. Northern Hemisphere observations are less seasonally biased, but nonetheless have been preferentially collected in the summer, so a comparable bias might also be expected for the global data. If anything, these estimates might be conservative since the Antonov et al. (2005) estimate could be low in the deep ocean if their averaging methods do not properly approximate trends where little or no data are available, particularly in the deep high-latitude regions of the ocean. These findings suggest that thermal expansion of the ocean could have been a larger contributor to twentieth-century global sea level rise than some recent budgets have supposed (e.g., Munk 2002; Nerem et al. 2006).

b. Transport change

The same calculations that indicate large-scale steric sea level rise can also be used to examine regional changes in dynamic topography associated with long-term shifts in geostrophic transport. Since salinity can play an important role in geostrophic transport in the Southern Ocean, these calculations can be thought of only as rough approximations. The trends found in this analysis amount to regional sea level changes of about ±0.1 to 3 mm $year^{-1}$. When dynamic height bins are used to average the data, this results in increased surface velocities on the southern side of the ACC (for dynamic height contours less than 1 dynamic meter) and decreased surface velocities on the northern flank of the ACC (between dynamic height contours of 1 and 1.4 dynamic meters), which would be consistent with a large-scale southward shift in the position of the ACC jets. Assuming that the ACC has an equivalent barotropic structure with an *e*-folding depth of 700 m (e.g., Gille 2003), the changes could be interpreted to suggest an approximate transport increase of $9 \pm 1 \times 10^6$ m^3 $century^{-1}$ between 0.6 and 1.0 dynamic meters, and a $9 \pm 1 \times 10^6$ m^3 $century^{-1}$ transport decrease between 1.0 and 1.2 dynamic meters. (Latitudinal bin averaging shows a similar pattern but does not resolve as much detail.) Because the ACC transport undergoes substantial high-frequency variability, this magnitude of regional transport trend would be extremely difficult to detect in the low-frequency observations currently available (as noted by Meredith and Hughes 2005). North of the ACC the equivalent barotropic assumption breaks down, so it is less clear how to translate surface dynamic height variations into transport trends.

6. Evaluating mechanisms

Changes in upper ocean heat content could be attributed either to changes in air–sea heat fluxes or to horizontal advection of heat within the ocean.[1] If the (20 to 27) × 10^{22} J Southern Hemisphere 70-yr increase in heat content were strictly the result of advective or diffusive processes within the ocean, the net increase in meridional heat transport across the equator and 60°S would need to have been (0.09 to 0.12) × 10^{15} W, roughly speaking an order of magnitude smaller than the estimated oceanic heat transport across the equator and well within uncertainties of oceanic heat transport

[1] Vertical entrainment of heat from the deep ocean could in principle also lead to changes in heat content within the top 1000 m; however, since the heat content changes are larger near the surface, entrainment could at best be a minor contributor.

estimates at either the equator or 60°S (Jayne and Marotzke 2002; Ganachaud and Wunsch 2003). While the formal uncertainties do not exclude oceanic heat advection as a source of the observed warming, the evidence that the warming is global in scope (e.g., Levitus et al. 2000, 2005a; Ishii et al. 2006; Bindoff et al. 2007) implies that on a hemispheric to global scale it is forced from the atmosphere.

To explain the Southern Hemisphere warming through air–sea exchange would require an average net heat input to the upper ocean between 0° and 60°S of 0.5 to 0.7 W m^{-2} over the 70-yr period from the 1930s to the present, or about 0.4 W m^{-2} using the trends from the 1950s to the present. This 0.4 to 0.7 W m^{-2} heat imbalance is small enough that it cannot be identified in climatological or reanalysis air–sea heat flux products. For example, annually averaged net surface heat fluxes for this region vary substantially, ranging from 8 (Kalnay et al. 1996) to 31 W m^{-2} (Josey et al. 1999), and regional differences can differ by as much as 50 W m^{-2} (Dong et al. 2007). Overall, the 0.4 to 0.7 W m^{-2} net heat flux to the ocean found here is roughly consistent with the 1993–2003 trend of 0.5 ± 0.18 W m^{-2} reported by Bindoff et al. (2007), and it exceeds the 0.2 W m^{-2} net heat flux to the top 700 m of the global ocean for the more comparable time period from 1955–2003 estimated by Levitus et al. (2005a). The discrepancy may be partly due to hemispheric differences: for the period 1940–99, using a model-based analysis method that discounts regions for which data are not available, Barnett et al. (2005) found substantially larger net surface heat fluxes (~0.5 W m^{-2}) into the Southern Hemisphere ocean compared with the Northern Hemisphere.

While the global increase in oceanic heat content can best be explained as a response to forcing from the atmosphere, the regional increase in heat content concentrated in the Southern Ocean can plausibly be explained either as a response to regional air–sea exchange or as a manifestation of oceanic heat advection. Since most of the observed subsurface warming is concentrated south of 30°S, this discussion will analyze processes that may govern the observed changes within the Southern Ocean, particularly in the region of the ACC. Bindoff and McDougall (1994) presented a framework for interpreting changes in water properties on isopycnal surfaces, distinguishing between the displacement of isopycnal surfaces with no change in water mass properties ("heave"), the addition of heat ("warming"), or the loss of salinity ("freshening"). Since salinity records are not reliable over the multidecade period used for this analysis, only changes in ocean temperature can be considered here, but, in analogy with Bindoff and McDougall (1994), a distinction can be drawn between warming (e.g., though air–sea heat exchange) and spatial displacement of water mass properties.[2]

First, we consider surface-driven warming. If heat simply diffused downward from the surface, then equal surface fluxes everywhere would imply roughly equal surface-intensified warming trends throughout the global ocean. As a simple test case for this study, a surface temperature anomaly of 10°C is allowed to diffuse downward at a rate $\kappa = 10^{-4}$ m^2 s^{-1} for 50 yr, following an approach similar to that used by Gille (2004). This framework explains about 40% of the rate of change in temperature below 200-m depth and north of the ACC (dynamic height contours between 1.2 and 2.4 dynamic meters in Fig. 7a), but it has little skill in the southern part of the domain.

The simple model suggesting that warming stems from vertical diffusion of course neglects much of our understanding of the meridional overturning circulation. Isopycnals tilt steeply across the ACC so that density surfaces that are 2000 m deep or deeper in the subtropics outcrop at the surface. In schematic representations of meridional overturning circulation (see, e.g., Speer et al. 2000), water upwells along these isopycnals to the surface, is carried northward by surface Ekman transport during which time the water exchanges heat with the atmosphere, and then sinks again to form Antarctic Intermediate Water or Subantarctic Mode Water. Thus, surface heat fluxes might be expected to produce warming patterns concentrated near the ocean surface in regions just north of the ACC, where intermediate water formation is most pronounced. Assuming this heat penetrates the ocean along isopycnal surfaces, then we expect to see subsurface warm patches extending downward toward the subtropical gyres. Several recent studies have found evidence for long-term changes in the temperature and salinity characteristics of Subantarctic Mode Water (Bindoff and Church 1992; Johnson and Orsi 1997; Wong et al. 1999), suggesting that air–sea fluxes can lead to subsurface warming patterns. However, much of the warming pattern shown in the upper panels of Fig. 7 implies warming within the top 1000 m of the ACC, which is not fully consistent with warming due to surface fluxes and associated intermediate water formation.

[2] For the study period, salinity effects are thought to play a less important role than temperature effects. Analyses of density from Southern Ocean Argo floats from the time period 2002–05 compared with older atlas data show a net shoaling of isopycnal surfaces, implying that the observed Southern Ocean warming is not salinity compensated (R. Karsten 2005, personal communication).

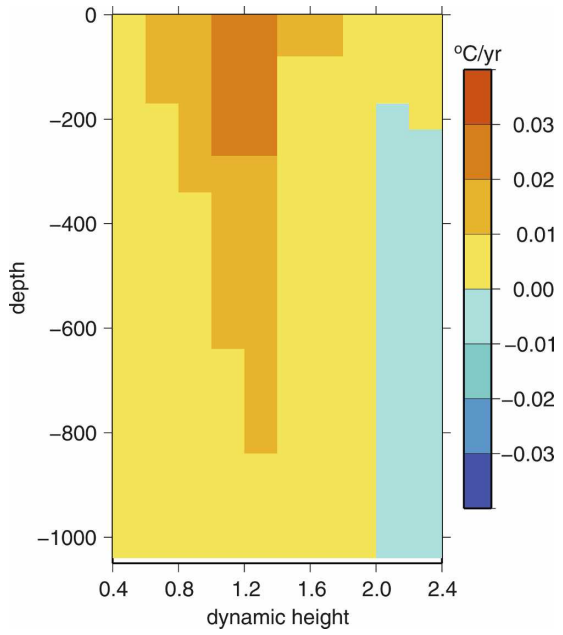

FIG. 8. Effective rate of change of temperature predicted if warming trends were entirely due to a poleward shift in oceanic features of 1° latitude every 40 yr. This pattern can be compared with the observed warming trend in the top left panel of Fig. 7.

An alternate possibility is that the warming is consistent with poleward displacement of warm water, analogous to heave. The ACC is defined by multiple jetlike frontal features that separate distinct water masses (Orsi et al. 1995) and meander in time (e.g., Gille 1994; Sprintall 2003). ACC jets are top-to-bottom features that are often described as being equivalent barotropic (Killworth 1992). Their variability shows strong vertical coherence (e.g., Lutjeharms 1982; Whitworth et al. 1991; Sokolov and Rintoul 2003). Since the jets correspond to strong north–south temperature gradients, ACC meandering can lead to anomalously warm or cold water at a given latitude. Figure 8 depicts the warming pattern that would be observed along dynamic height contours if all temperature surfaces were displaced poleward at a rate of 1° latitude every 40 yr. North of the ACC, this pattern differs substantially from the top left panel of Fig. 7 over much of the ocean but agrees well between 0.4 and 1.2 dynamic meters. In this range the poleward shift of oceanic features is able to explain 87% of the temperature trend below 200 m in Fig. 7, while vertical diffusion of a temperature anomaly would explain no more than 7% of the trend. This implies that that much of the long-term trend in the ACC is consistent with a poleward displacement of frontal features [though these data do not preclude the possibility that water masses have changed in ways that cannot be detected using temperature data alone, as suggested by, e.g., Aoki et al. (2005).] A number of regional observational studies based on more limited data have reached similar conclusions (Swift 1995; Aoki et al. 2003; Sprintall 2008). For example, in the Indian Ocean sector, Aoki et al. (2003) found a warming trend consistent with a 0.3° to 0.6° poleward shift of the vertical temperature patterns over 26 yr.

What could drive this possible poleward frontal displacement? On time scales shorter than 3 yr, Dong et al. (2006) found that meridional displacements of the latitude of the maximum wind over the Southern Ocean were statistically coherent with meridional displacements of the ACC's Polar Front (PF), which they identified from satellite microwave sea surface temperature data. In their analysis, the predominant phase relationship between wind stress and PF position is slightly negative, implying that changes in wind typically drive changes in the PF position. Assuming that the pattern of variability found by Dong et al. (2006) applies for time scales longer than a few years, then it has clear implications for the long-term trends in the Southern Ocean. Historic wind records are minimal for the Southern Hemisphere prior to 1970 (Kalnay et al. 1996). However, available observations generally suggest that the dominant mode of wind variability, the Southern Annular Mode, has strengthened over the past few decades, likely driven by changes in greenhouse gas and stratospheric ozone concentrations, and that the winds have correspondingly shifted poleward (e.g., Gong and Wang 1999; Thompson et al. 2000; Thompson and Solomon 2002; Gillett and Thompson 2003; Marshall 2003; Thompson et al. 2005; Arblaster and Meehl 2006; Cai and Cowan 2007). This strengthening wind appears to have driven corresponding increases in ACC transport (Meredith et al. 2004; Cai 2006). Recent coupled climate simulations carried out as part of the Intergovernmental Panel on Climate Change suggest that anthropogenic climate change is responsible for the poleward shift in the winds driving the ACC (Yin 2005) and for corresponding shifts in the position and strength of the modeled ACC (Cai et al. 2005; Fyfe and Saenko 2005, 2006). Model analyses also suggest that strengthening midlatitude gyre circulation may advect more heat southward (Cai and Cowan 2007) and that related changes in isopycnal tilts may induce baroclinic instability that strengthens poleward eddy heat fluxes across the ACC (Meredith and Hogg 2006; Fyfe et al. 2007; Hogg et al. 2008). Like the modeled ocean, the observed ocean warming may also be driven, at least in part, by poleward shifts in the Southern Hemisphere westerlies linked to anthropogenic climate change.

7. Summary and discussion

This study has compared historic measurements of ocean temperature in the top 1000 m of the Southern Hemisphere with measurements collected during the 1990s. Data are drawn from the *World Ocean Database 2005*, the Argo data, and the 1990s PALACE float records. They include observations from bottle data, CTDs, XBTs, and profiling floats. Here analysis has been limited to summer data to reduce seasonal sampling biases, and a basic assumption has been made that temperature trends in places with no observations should resemble temperature trends in statistically similar regions where observations have been collected. Overall, the results indicate that the Southern Hemisphere ocean has warmed substantially since the 1930s. Some 80% of this warming is concentrated south of 30°S where it is evident at all depths. Observations are also sparsest in this latitude range. Estimates of the exact amount of warming that has occurred therefore depend on the details of the assumptions made about temperature trends in regions where no observations are available, as studies based on numerical climate simulations (e.g., Gregory et al. 2004; AchutaRao et al. 2006) and other hydrographic analyses (Gouretski and Koltermann 2007) have also shown.

The Southern Ocean trend is largely consistent with a long-term poleward migration of the ACC, although available data do not exclude other mechanisms including increased heat flux from the atmosphere within the Southern Ocean or increased poleward eddy heat flux. The findings suggest that warmer water frontal features could be perhaps a few hundred kilometers closer to Antarctica now than they were 50 yr ago (at least in locations where the ACC path is not entirely topographically constrained). The implications of this for the climate system are unclear, but potentially provide a source of warm water to feed a reported long-term warming of the Weddell Sea (Robertson et al. 2002; Fahrbach et al. 2004).[3] In addition, at longitudes where the ACC fronts are farthest south, just west of Drake Passage, a poleward displacement of the ACC frontal features (or a strengthening and/or warming of the southernmost jet of the ACC) could bring anomalously warm water into contact with the ice shelves, potentially contributing to the rapid melting observed in this region (e.g., Rignot 1998; Wingham et al. 1998; Shepherd et al. 2001, 2004). Finally, the observed warming has implications for global meridional overturning circulation, though the exact effect is still subject to some speculation. If the changes are dominated by increased upper ocean stratification, then warming patterns may cap off the upper ocean and inhibit further deep ocean storage of heat and greenhouse gases (e.g., Caldeira and Duffy 2000). Alternatively, Russell et al. (2006) suggested that, as Southern Hemisphere westerlies shift poleward, they might expose a greater volume of water to contact with the atmosphere (despite expected increases in upper ocean stratification) and that this could ultimately allow still greater ocean storage of heat and greenhouse gases and continued warming of the Southern Hemisphere ocean.

Acknowledgments. PALACE float data were provided by Russ Davis (Scripps Institution of Oceanography). The Argo data were collected and made freely available by the international Argo Project and the national programs that contribute to it (www.argo.ucsd.edu; argo.jcommops.org). Argo is a pilot program of the Global Ocean Observing System. The *World Ocean Database 2005* is available from www.nodc.noaa.gov/OC5/WOD05/prwod05.html. Discussions with numerous colleagues, including Russ Davis, John Gilson, Syd Levitus, Joe Reid, Dean Roemmich, and Josh Willis, and comments from Mike Meredith and the anonymous reviewers have all proved immensely helpful. This research was supported by the National Science Foundation under Grant OCE-9985203/OCE-0049066.

APPENDIX

Assessing Data Biases

Inherent differences between the different data types were assessed by carrying out nearest neighbor comparisons for November–March observations collected during the 1990s. The comparisons are summarized in Table A1 for two depths: 20 and 500 m. Uncertainties reported in Table A1 are standard errors, computed from the standard deviation divided by $\sqrt{N_{\text{eff}}}$, where $N_{\text{eff}} = N_1N_2/(N_1 + N_2)$ and N_1 and N_2 represent the number of observations used from each data type. Since observations may be paired with multiple adjacent observations, the total number of pairs used to compute the mean and standard deviation is typically much greater than either N_1 or N_2. The temperature comparisons reported in Table A1 were also carried out at other depths and using alternate latitude bands and seasonal constraints. While the details of the temperature differences vary, comparisons consistently show

[3] However, Weddell Sea trends are not entirely monotonic: Fahrbach et al. (2004) show evidence for a recent cooling trend in the Weddell Sea Warm Deep Water, but on a time scale too short to be resolved by the decadal temporal resolution considered here.

TABLE A1. Temperature differences (°C) between observations collected using different measurement techniques, within 220 km geographically. Here positive values indicate that the quantity identified in the column heading is warmer than the quantity identified in the row label. MBT refers to mechanical bathythermograph observations, and OSD to bottle data, following World Ocean Atlas nomenclature conventions. Results are reported based on World Ocean Atlas standard level depths, and PALACE and Argo profiles have been interpolated to these depths. Temperature differences should form an antisymmetric matrix. Only the upper right triangle is reported here. Values in bold font indicate average temperature differences that exceed three times the standard error.

Method	PALACE	MBT	CTD	XBT	OSD	Argo
			20 m			
PALACE	0.00 ± 0.05	0.21 ± 0.20	**0.23 ± 0.07**	**0.67 ± 0.04**	**1.08 ± 0.12**	−0.21 ± 0.40
MBT		0.00 ± 0.17	**0.58 ± 0.12**	**0.34 ± 0.10**	**2.14 ± 0.26**	0.23 ± 0.16
CTD			0.00 ± 0.03	**0.22 ± 0.03**	**0.16 ± 0.05**	0.33 ± 0.19
XBT				0.00 ± 0.01	−0.01 ± 0.05	−0.13 ± 0.10
OSD					0.00 ± 0.09	−0.28 ± 0.21
Argo						0.00 ± 0.15
			500 m			
PALACE	0.00 ± 0.03	0.01 ± 0.05	0.06 ± 0.04	**0.17 ± 0.03**	0.03 ± 0.08	−0.06 ± 0.10
MBT		0.00 ± 0.03	−0.13 ± 0.04	0.10 ± 0.03	0.09 ± 0.05	−0.03 ± 0.13
CTD			0.00 ± 0.01	0.03 ± 0.01	**0.16 ± 0.04**	**0.13 ± 0.04**
XBT				0.00 ± 0.01	−0.11 ± 0.03	−0.02 ± 0.03
OSD					0.00 ± 0.04	−0.03 ± 0.07
Argo						0.00 ± 0.03

that PALACE, CTD, and Argo data tend to be slightly cooler than XBT, and Argo temperatures. Gouretski and Koltermann (2007) reported warm biases in MBT and XBT data, not surprisingly since neither data type was designed to meet the requirements of long-term climate studies. For XBT data, they found a mean warm bias in XBT data relative to CTD data of 0.28°C, with largest differences between 50- and 250-m depth. This bias has been attributed to errors in the determination of fall rate, but improved fall rates are not yet available (Willis et al. 2008, manuscript submitted to *J. Atmos. Oceanic Technol.*). A similar bias shows up in this analysis, although it is sensitive to the specific choice of data for the comparisons: If summer is defined to extend from October to March (not shown), then this methodology suggests no statistically significant temperature difference between 1990s CTD and XBT profiles.

Modern floats and research vessels normally operate around the clock, so in principle observations should be collected uniformly throughout the day. However, some types of data were collected primarily during local daytime. For example, ships of the former Soviet Union made most of the 1990s MBT observations during daytime. Diurnal temperature variability is expected to be detectable within the mixed layer to depths O(100 m) (e.g., Cronin and McPhaden 1997), so a daytime sampling bias could bias estimates of long-term temperature trends. Limiting the analysis to only local daytime observations would reduce possible temperature bias but also decrease the number of observations available for this analysis. Because MBT data differ substantially from other measurements collected during the 1990s and because historically they are thought to be less accurate than other measurement types, MBT data have been excluded from the remainder of this analysis.

As shown in Table A1, at 500-m depth, in most cases instruments agree within three standard errors, while at 20-m depth, for 8 of the 15 instrument pairs, temperatures differ by more than three standard deviations and are marked in bold. If the mean ocean temperature differences had Gaussian distributions, 99.7% of the data types would be expected to agree within ±three standard errors. However, as Sura et al. (2006) have shown, ocean surface temperatures can have non-Gaussian distributions, implying that the mean statistics may converge rather slowly to Gaussianity, particularly at the ocean surface. Thus, the disagreement does not necessarily imply that one observation type is biased relative to another.

REFERENCES

AchutaRao, K. M., B. D. Santer, P. J. Gleckler, K. E. Taylor, D. W. Pierce, T. P. Barnett, and T. M. L. Wigley, 2006: Variability of ocean heat uptake: Reconciling observations and models. *J. Geophys. Res.,* **111,** C05019, doi:10.1029/2005JC003136.

Antonov, J. I., S. Levitus, and T. P. Boyer, 2002: Steric sea level variations during 1957–1994: Importance of salinity. *J. Geophys. Res.,* **107,** 8013, doi:10.1029/2001/JC000964.

——, ——, and ——, 2005: Thermosteric sea level rise, 1955–2003. *Geophys. Res. Lett.,* **32,** L12602, doi:10.1029/2005GL023112.

Aoki, S., M. Yoritaka, and A. Masuyama, 2003: Multidecadal warming of subsurface temperature in the Indian sector of the Southern Ocean. *J. Geophys. Res.,* **108,** 8081, doi:10.1029/2000JC000307.

——, N. L. Bindoff, and J. A. Church, 2005: Interdecadal water mass changes in the Southern Ocean between 30°E and 160°E. *Geophys. Res. Lett.,* **32,** L07607, doi:10.1029/2004GL022220.

Arbic, B. K., and W. B. Owens, 2001: Climatic warming of Atlantic intermediate waters. *J. Climate,* **14,** 4091–4108.

Arblaster, J. M., and G. A. Meehl, 2006: Contributions of external forcings to Southern Annular Mode trends. *J. Climate,* **19,** 2896–2905.

Banks, H., and R. Wood, 2002: Where to look for anthropogenic climate change in the ocean. *J. Climate,* **15,** 879–891.

Barnett, T. P., D. W. Pierce, K. M. AchutaRao, P. J. Gleckler, B. D. Santer, J. M. Gregory, and W. M. Washington, 2005: Penetration of human-induced warming into the world's oceans. *Science,* **309,** 284–287.

Bindoff, N. L., and J. Church, 1992: Warming of the water column in the southwest Pacific Ocean. *Nature,* **357,** 59–62.

——, and T. J. McDougall, 1994: Diagnosing climate change and ocean ventilation using hydrographic data. *J. Phys. Oceanogr.,* **24,** 1137–1152.

——, and Coauthors, 2007: Observations: Oceanic climate change and sea level. *Climate Change 2007: The Physical Science Basis,* S. Solomon et al., Eds., Cambridge University Press, 385–432.

Boyer, T. P., and Coauthors, 2006: *World Ocean Database 2005.* NOAA Atlas NESDIS 60, U.S. Government Printing Office, 190 pp.

Bretherton, F. P., R. E. Davis, and C. B. Fandry, 1976: A technique for objective analysis and design of oceanographic experiments applied to MODE-73. *Deep-Sea Res.,* **23,** 559–582.

Cai, W., 2006: Antarctic ozone depletion causes an intensification of the Southern Ocean super-gyre circulation. *Geophys. Res. Lett.,* **33,** L03712, doi:10.1029/2005GL024911.

——, and T. Cowan, 2007: Trends in Southern Hemisphere circulation in IPCC AR4 models over 1950–99: Ozone depletion versus greenhouse forcing. *J. Climate,* **20,** 681–693.

——, G. Shi, T. Cowan, D. Bi, and J. Ribbe, 2005: The response of the Southern Annular Mode, the East Australian Current, and the southern mid-latitude ocean circulation to global warming. *Geophys. Res. Lett.,* **32,** L23706, doi:10.1029/2005GL024701.

Caldeira, K., and P. B. Duffy, 2000: The role of the Southern Ocean in uptake and storage of anthropogenic carbon dioxide. *Science,* **287,** 620–622.

Capotondi, A., M. A. Alexander, C. Deser, and A. Miller, 2005: Low-frequency pycnocline variability in the Northeast Pacific. *J. Phys. Oceanogr.,* **35,** 1403–1420.

Cazenave, A., and R. S. Nerem, 2004: Present-day sea level change: Observations and causes. *Rev. Geophys.,* **42,** RG3001, doi:10.1029/2003RG000139.

Chapman, W. L., and J. E. Walsh, 2007: A synthesis of Antarctic temperatures. *J. Climate,* **20,** 4096–4117.

Church, J. A., and N. J. White, 2006: A 20th century acceleration in global sea-level rise. *Geophys. Res. Lett.,* **33,** L01602, doi:10.1029/2005GL024826.

——, J. M. Gregory, P. Huybrechts, M. Kuhn, K. Lambeck, M. T. Nhuan, D. Qin, and P. L. Woodworm, 2001: Changes in sea level. *Climate Change 2001: The Scientific Basis,* J. T. Houghton et al., Eds., Cambridge University Press, 639–693.

Conkright, M. E., and Coauthors, 2002: *Introduction.* Vol. 1, *World Ocean Atlas 2001,* NOAA Atlas NESDIS 42, 160 pp.

Cronin, M. F., and M. J. McPhaden, 1997: The upper ocean heat balance in the western equatorial Pacific warm pool during September–December 1992. *J. Geophys. Res.,* **102,** 8533–8553.

Davis, R. E., 1998: Preliminary results from directly measuring middepth circulation in the tropical and South Pacific. *J. Geophys. Res.,* **103,** 24 619–24 639.

——, 2005: Intermediate-depth circulation of the Indian and South Pacific Oceans measured by autonomous floats. *J. Phys. Oceanogr.,* **35,** 683–707.

——, D. C. Webb, L. A. Regier, and J. Dufour, 1992: The Autonomous Lagrangian Circulation Explorer (ALACE). *J. Atmos. Oceanic Technol.,* **9,** 264–285.

——, P. D. Killworth, and J. R. Blundell, 1996: Comparison of Autonomous Lagrangian Circulation Explorer and Fine Resolution Antarctic Model results in the South Atlantic. *J. Geophys. Res.,* **101,** 855–884.

——, J. T. Sherman, and J. Dufour, 2001: Profiling ALACEs and other advances in autonomous subsurface floats. *J. Atmos. Oceanic Technol.,* **18,** 982–993.

Dong, S., J. Sprintall, and S. T. Gille, 2006: Location of the polar front from AMSR-E satellite sea surface temperature measurements. *J. Phys. Oceanogr.,* **36,** 2075–2089.

——, S. T. Gille, and J. Sprintall, 2007: An assessment of the Southern Ocean mixed layer heat budget. *J. Climate,* **20,** 4425–4442.

Doran, P. T., and Coauthors, 2002: Antarctic climate cooling and terrestrial ecosystem response. *Nature,* **415,** 517–520.

Fahrbach, E., M. Hoppema, G. Rohardt, M. Schroder, and A. Wisotzki, 2004: Decadal-scale variation of water mass properties in the deep Weddell Sea. *Ocean Dyn.,* **54,** 77–91.

Fyfe, J. C., and O. A. Saenko, 2005: Human-induced change in the Antarctic Circumpolar Current. *J. Climate,* **18,** 3068–3073.

——, and ——, 2006: Simulated changes in the extratropical Southern Hemisphere winds and currents. *Geophys. Res. Lett.,* **33,** L06701, doi:10.1029/2005GL025332.

——, ——, K. Zickfeld, M. Eby, and A. J. Weaver, 2007: The role of poleward-intensifying winds on Southern Ocean warming. *J. Climate,* **20,** 5391–5400.

Ganachaud, A., and C. Wunsch, 2003: Large-scale ocean heat and freshwater transports during the World Ocean Circulation Experiment. *J. Climate,* **16,** 696–705.

Gille, S. T., 1994: Mean sea surface height of the Antarctic Circumpolar Current from Geosat data: Method and application. *J. Geophys. Res.,* **99,** 18 255–18 273.

——, 2002: Warming of the Southern Ocean since the 1950s. *Science,* **295,** 1275–1277.

——, 2003: Float observations of the Southern Ocean. Part I: Estimating mean fields, bottom velocities, and topographic steering. *J. Phys. Oceanogr.,* **33,** 1167–1181.

——, 2004: How non-linearities in the equation of state of sea water can confound estimates of steric sea level change. *J. Geophys. Res.,* **109,** C03005, doi:10.1029/2003JC002012.

Gillett, N. P., and D. W. J. Thompson, 2003: Simulation of recent Southern Hemisphere climate change. *Science,* **302,** 273–275.

Gong, D., and S. Wang, 1999: Definition of Antarctic Oscillation index. *Geophys. Res. Lett.,* **26,** 459–462.

Gouretski, V. V., and K. Jancke, 1998: A new climatology for the world ocean. WOCE Hydrographic Program Special Analysis Centre Tech. Rep. 3, WOCE Rep. 162/98, Hamburg, Germany, 40 pp.

——, and K. P. Koltermann, 2007: How much is the ocean really

warming? *Geophys. Res. Lett.,* **34,** L01610, doi:10.1029/2006GL027834.

Gregory, J. M., H. T. Banks, P. A. Stott, J. A. Lowe, and M. D. Palmer, 2004: Simulated and observed decadal variability in ocean heat content. *Geophys. Res. Lett.,* **31,** L15312, doi:10.1029/2004GL020258.

Harrison, D. E., and M. Carson, 2007: Is the world ocean warming? Upper-ocean temperature trends: 1950–2000. *J. Phys. Oceanogr.,* **37,** 174–187.

Hogg, A. M., M. P. Meredith, J. R. Blundell, and C. Wilson, 2008: Eddy heat flux in the Southern Ocean: Response to variable wind forcing. *J. Climate,* **21,** 608–620.

Ishii, M., M. Kimoto, K. Sakamoto, and S. I. Iwasaki, 2006: Steric sea level changes estimated from historical ocean subsurface temperature and salinity analyses. *J. Oceanogr.,* **62,** 155–170.

Jacobs, S., 2006: Observations of change in the Southern Ocean. *Philos. Trans. Roy. Soc. London,* **A364,** 1657–1681.

Jayne, S. R., and J. Marotzke, 2002: The oceanic eddy heat transport. *J. Phys. Oceanogr.,* **32,** 3328–3345.

Johnson, D. R., and Coauthors, 2006: *World Ocean Database 2005 Documentation.* NODC Internal Rep. 18, U.S. Government Printing Office, 163 pp. [Available online at http://www.nodc.noaa.gov/OC5/WOD05/docwod05.html.]

Johnson, G. C., and A. H. Orsi, 1997: Southwest Pacific Ocean water mass changes between 1968/69 and 1990/91. *J. Climate,* **10,** 306–316.

Josey, S. A., E. C. Kent, and P. K. Taylor, 1999: New insights into the ocean heat budget closure problem from analysis of the SOC air–sea flux climatology. *J. Climate,* **12,** 2856–2880.

Kalnay, E., and Coauthors, 1996: The NCEP/NCAR 40-Year Reanalysis Project. *Bull. Amer. Meteor. Soc.,* **77,** 437–471.

Killworth, P. D., 1992: An equivalent-barotropic mode in the Fine Resolution Antarctic Model. *J. Phys. Oceanogr.,* **22,** 1379–1387.

Lavender, K. L., R. E. Davis, and W. B. Owens, 2000: Mid-depth recirculation observed in the interior Labrador and Irminger seas by direct velocity measurements. *Nature,* **407,** 66–69.

Levitus, S., J. I. Antonov, T. P. Boyer, and C. Stephens, 2000: Warming of the world ocean. *Science,* **287,** 2225–2229.

——, ——, J. L. Wang, T. L. Delworth, K. W. Dixon, and A. J. Broccoli, 2001: Anthropogenic warming of earth's climate system. *Science,* **292,** 267–270.

——, J. Antonov, and T. Boyer, 2005a: Warming of the world ocean, 1955–2003. *Geophys. Res. Lett.,* **32,** L02604, doi:10.1029/2004GL021592.

——, ——, ——, H. E. Garcia, and R. A. Locarnini, 2005b: Linear trends of zonally averaged thermosteric, halosteric, and total steric sea level for individual ocean basins and the world ocean, (1955–1959)–(1994–1998). *Geophys. Res. Lett.,* **32,** L16601, doi:10.1029/2005GL023761.

Locarnini, R. A., A. V. Mishonov, J. I. Antonov, T. P. Boyer, and H. E. Garcia, 2006: *Temperature*. Vol. 1, *World Ocean Atlas 2005,* NOAA Atlas NESDIS 61, 182 pp.

Lutjeharms, J. R. E., 1982: Baroclinic volume transport in the Southern Ocean. *J. Phys. Oceanogr.,* **12,** 3–7.

Marshall, G. J., 2003: Trends in the Southern Annular Mode from observations and reanalyses. *J. Climate,* **16,** 4134–4143.

Meredith, M. P., and C. Hughes, 2005: On the sampling timescale required to reliably monitor interannual variability in the Antarctic circumpolar transport. *Geophys. Res. Lett.,* **32,** L03609, doi:10.1029/2004GL022086.

——, and J. C. King, 2005: Rapid climate change in the ocean west of the Antarctic Peninsula during the second half of the 20th century. *Geophys. Res. Lett.,* **32,** L19604, doi:10.1029/2005GL024042.

——, and A. M. Hogg, 2006: Circumpolar response of Southern Ocean eddy activity to a change in the Southern Annular Mode. *Geophys. Res. Lett.,* **33,** L16608, doi:10.1029/2006GL026499.

——, P. L. Woodworm, C. W. Hughes, and V. Stepanov, 2004: Changes in the ocean transport through Drake Passage during the 1980s and 1990s, forced by changes in the Southern Annular Mode. *Geophys. Res. Lett.,* **31,** L21305, doi:10.1029/2004GL02116.

Munk, W., 2002: Twentieth century sea level: An enigma. *Proc. Natl. Acad. Sci. USA,* **99,** 6550–6555.

——, 2003: Ocean freshening, sea level rising. *Science,* **300,** 2041–2042.

Nerem, R. S., E. Leuliette, and A. Cazenave, 2006: Present-day sea-level change: A review. *Compt. Rend. Geosci.,* **338,** 1077–1083.

Orsi, A. H., T. Whitworth III, and W. D. Nowlin Jr., 1995: On the meridional extent and fronts of the Antarctic Circumpolar Current. *Deep-Sea Res. I,* **42,** 641–673.

Pickard, G. L., and W. J. Emery, 1990: *Descriptive Physical Oceanography*. 5th ed. Butterworth-Heinemann, 320 pp.

Pritchard, H. D., and D. G. Vaughan, 2007: Widespread acceleration of tidewater glaciers on the Antarctic Peninsula. *J. Geophys. Res.,* **112,** F03S29, doi:10.1029/2006JF000597.

Reynolds, R. W., and T. W. Smith, 1994: Improved global sea surface temperature analyses using optimum interpolation. *J. Climate,* **7,** 929–948.

Rignot, E. J., 1998: Fast recession of a West Antarctic Glacier. *Science,* **281,** 549–551.

——, and S. S. Jacobs, 2002: Rapid bottom melting widespread near Antarctic ice sheet grounding lines. *Science,* **296,** 2020–2023.

Robertson, R., M. Visbeck, A. L. Gordon, and E. Fahrbach, 2002: Long-term temperature trends in the deep waters of the Weddell Sea. *Deep-Sea Res. II,* **49,** 4791–4806.

Roemmich, D., and Coauthors, 2001: Argo: The global array of profiling floats. *Observing the Oceans in the 21st Century,* C. J. Koblinsky and N. R. Smith, Eds., GODAE Project Office and Bureau of Meteorology, 248–258.

Russell, J. L., K. W. Dixon, A. Gnanadesikan, R. J. Stouffer, and J. R. Toggweiler, 2006: The Southern Hemisphere westerlies in a warming world: Propping open the door to the deep ocean. *J. Climate,* **19,** 6382–6390.

Sabine, C. L., and Coauthors, 2004: The oceanic sink for anthropogenic CO_2. *Science,* **305,** 367–371.

Saunders, P. M., and N. P. Fofonoff, 1976: Conversion of pressure to depth in the ocean. *Deep-Sea Res.,* **23,** 109–111.

Shepherd, A., D. J. Wingham, J. A. D. Mansley, and H. F. J. Corr, 2001: Inland thinning of Pine Island Glacier, West Antarctica. *Science,* **291,** 862–864.

——, ——, and E. Rignot, 2004: Warm ocean is eroding West Antarctic Ice Sheet. *Geophys. Res. Lett.,* **31,** L23402, doi:10.1029/2004GL021106.

Smith, T. M., and R. W. Reynolds, 2004: Improved extended reconstruction of SST (1854–1997). *J. Climate,* **17,** 2466–2477.

Sokolov, S., and S. R. Rintoul, 2003: Subsurface structure of interannual temperature anomalies in the Australian sector of the Southern Ocean. *J. Geophys. Res.,* **108,** 3285, doi:10.1029/2002JC001494.

Speer, K., S. R. Rintoul, and B. Sloyan, 2000: The diabatic Deacon cell. *J. Phys. Oceanogr.,* **30,** 3212–3222.

Sprintall, J., 2003: Seasonal to interannual upper ocean variability in the Drake Passage. *J. Mar. Res.,* **61,** 27–57.

——, 2008: Long term trends and interannual variability of temperature in Drake Passage. *Prog. Oceanogr.,* **77,** 316–330.

Sura, P., M. Newman, and M. Alexander, 2006: Daily to decadal sea surface temperature variability driven by state-dependent stochastic heat fluxes. *J. Phys. Oceanogr.,* **36,** 1940–1958.

Swift, J. H., 1995: Comparing WOCE and historical temperatures in the deep southeast Pacific. *International WOCE Newsletter,* No. 18, WOCE International Project Office, Southampton, United Kingdom, 15–17.

Thompson, D. W. J., and S. Solomon, 2002: Interpretation of recent Southern Hemisphere climate change. *Science,* **296,** 895–899.

——, J. M. Wallace, and G. C. Hegerl, 2000: Annular modes in the extratropical circulation. Part II: Trends. *J. Climate,* **13,** 1018–1036.

——, M. P. Baldwin, and S. Solomon, 2005: Stratosphere–troposphere coupling in the Southern Hemisphere. *J. Atmos. Sci.,* **62,** 708–715.

Vaughan, D. G., and C. S. M. Doake, 1996: Recent atmospheric warming and retreat of ice shelves on the Antarctic Peninsula. *Nature,* **379,** 328–331.

——, G. J. Marshall, W. M. Connolley, J. C. King, and R. Mulvaney, 2001: Climate change: Devil in the detail. *Science,* **293,** 1777–1779.

Wainer, L., A. Taschetto, B. Otto-Bliesner, and E. Brady, 2004: A numerical study of the impact of greenhouse gases on the South Atlantic Ocean climatology. *Climatic Change,* **66,** 163–189.

Whitworth, I. T., R. D. Pillsbury, M. I. Moore, and R. F. Weiss, 1991: Observations of the Antarctic Circumpolar Current and deep boundary current in the southwest Atlantic. *J. Geophys. Res.,* **96,** 15 105–15 118.

Wingham, D. J., A. J. Ridout, R. Scharroo, R. J. Arthern, and C. K. Shum, 1998: Antarctic elevation change from 1992 to 1996. *Science,* **282,** 456–458.

Wong, A. P. S., N. L. Bindoff, and J. A. Church, 1999: Large-scale freshening of intermediate waters in the Pacific and Indian Oceans. *Nature,* **400,** 440–443.

——, ——, and ——, 2001: Freshwater and heat changes in the North and South Pacific Oceans between the 1960s and 1985–94. *J. Climate,* **14,** 1613–1633.

Yin, J. H., 2005: A consistent poleward shift of the storm tracks in simulations of 21st century climate change. *Geophys. Res. Lett.,* **32,** L18701, doi:10.1029/2005GL023684.